International Journal of Pharmaceutics 392 (2010) 20–28

Contents lists available at ScienceDirect

International Journal of Pharmaceutics

journal homepage: www.elsevier.com/locate/ijpharm

Active and passive tumor targeting of a novel poorly soluble cyclin dependent kinase inhibitor, JNJ-7706621

Fabienne Danhier[a], Bernard Ucakar[a], Nicolas Magotteaux[a], Marcus E. Brewster[b], Véronique Préat[a,*]

[a] Université Catholique de Louvain, Louvain Drug Institute, Avenue Mounier UCL 7320, B-1200 Brussels, Belgium
[b] Johnson and Johnson, Pharmaceutical Research and Development, Division of Janssen Pharmaceutica, 2340 Beerse, Belgium

ARTICLE INFO

Article history:
Received 17 December 2009
Received in revised form 2 March 2010
Accepted 4 March 2010
Available online 11 March 2010

Keywords:
Polymeric micelles
PLGA nanoparticles
RGD
CDK inhibitor
Tumor targeting

ABSTRACT

The anti-cancer cyclin dependent kinase (CDK) inhibitors are poorly soluble drugs. The aims of this work were (i) to formulate a novel CDK inhibitor, JNJ-7706621, in polymeric micelles and nanoparticles, (ii) to compare passive and active targeting on tumor growth and (iii) to evaluate the potential synergy of JNJ-7706621 with Paclitaxel. Therefore, JNJ-7706621 was encapsulated in self-assembling diblock copolymers made up of ε-caprolactone (CL) and trimethylene carbonate (TMC) (PEG-p-(CL-*co*-TMC)) polymeric micelles and in (poly(lactide-co-glycolide)) (PLGA)-based PEGylated nanoparticles (passive targeting) as well as in RGD-grafted nanoparticles (active targeting). In vivo, the transplantable liver tumor growth was more decreased by active targeting with RGD-grafted nanoparticles than by passive targeting with micelles or ungrafted nanoparticles. Moreover, a synergy between JNJ-7706621 and Paclitaxel was demonstrated. Therefore, active targeting of JNJ-7706621-loaded nanocarriers may be considered as an effective anti-cancer drug delivery system for cancer chemotherapy, particularly in combination with Paclitaxel.

1. Introduction

Cyclin dependent kinases (CDKs) control cell growth by regulating the progression of cells through the cell cycle. This process is regulated by the coordinated action of CDKs in association with their specific regulatory cyclin proteins. Each step in the cell cycle is regulated by a distinct and specific CDK. The combination of catalytic kinase subunits (such as CDK1, CDK2, CDK4 or CDK6) with regulatory cyclin subunits (such as cyclin A, B, D1, D2, D3 or E) results in the assembly of functionally distinct kinase complexes (Emanuel et al., 2005). Over-expression of CDK1 and CDK4 has been reported in a large variety of tumors. Therefore, selective inhibition of CDKs may limit the progression of a tumor cell through the cell cycle and facilitate the induction of apoptotic pathways. Most current anti-mitotic anti-cancer drugs have undesirable side effects on cells. CDK inhibitors have the potential to arrest cell growth with fewer side effects and may also avoid the problem of multidrug resistance (Lapenna and Giordano, 2009; Zhang et al., 2009).

JNJ-7706621 (Fig. 1) is a 1,2,4-triazole-3,5-diamine derivative that inhibits CDK activity and is being developed as an anti-tumor agent. JNJ-7706621 is a potent inhibitor of CDK1, CDK2 and to lesser extent, CDK4 activity (Lin et al., 2005). JNJ-7706621 blocks progression of human cancer cells through the cell cycle causing an accumulation of cells in the G_2/M phase, preventing cells from entering mitosis and activating apoptosis. CDK inhibitors, including JNJ-7706621, are poorly soluble in aqueous medium (17 μg/ml) (Emanuel et al., 2005). Therefore, the current challenge is to formulate JNJ-7706621 for the intravenous route in a non-toxic vehicle.

The percentage of apoptotic cells as well as the degree of cytotoxicity induced by CDK inhibitors could significantly be increased by treatment of tumor cells with cytostatic drugs that are known to induce apoptosis of tumor cells in all phases of the cell cycle (Sedlacek, 2001; Schwartz et al., 2002). More particularly, flavopiridol, a CDK inhibitor developed by Sanofi-Aventis, has been shown to act in synergy with several cytostatics including Paclitaxel (PTX), offering an attractive clinical treatment opportunity. PTX is an effective anti-cancer drug active against a wide variety of tumors, including ovarian carcinoma, metastatic breast cancer, head and neck cancers and non-small lung cancer (Schiff and Horwitz, 1980). PTX is currently formulated (Taxol®) at the concentration of 6 mg/ml dissolved in mixture of Cremophor® EL (polyethoxylated caster oil) and ethanol (50:50, v/v) (Nicolaou et al., 2009).

Polymeric micelles (Fig. 2) are arranged in a spheroidal structure with hydrophobic core which increases the solubility of poorly water-soluble drugs, and the hydrophilic corona which allows for a long circulation time of the drug by preventing the interactions between the core and the blood components. These systems are dynamic and have a size usually below 50 nm (Kwon, 2002). Due to their prolonged circulation time, polymeric micelles are able

* Corresponding author. Tel.: +32 2 7647320; fax: +32 2 7647398.
E-mail address: veronique.preat@uclouvain.be (V. Préat).

0378-5173/$ – see front matter © 2010 Elsevier B.V. All rights reserved.
doi:10.1016/j.ijpharm.2010.03.018

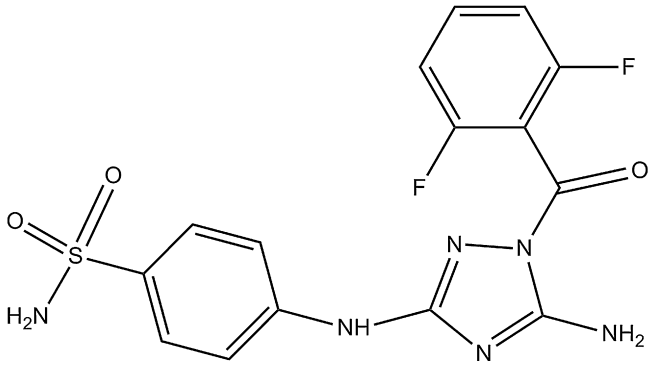

Fig. 1. Chemical structure of JNJ-7706621, 1-(2′,6′-difluorobenzoyl)-5-amino-3-(4′aminosulfonylanilino)-1,2,4-triazole.

to accumulate at certain biological sites characterized by vascular abnormalities, such as tumors, through the enhanced permeation and retention (EPR) effect (Maeda et al., 2009).

Nanoparticles (Fig. 2) are solid and spherical structures, ranging around 100 nm in size, in which drugs are encapsulated within the polymeric matrix (Byrne et al., 2008; Pirollo and Chang, 2008). Nanoparticles can also escape from the vasculature through the leaky endothelial tissue that surrounds the tumor and then accumulate in certain solid tumors by the EPR effect (Maeda et al., 2009). This phenomenon is called "*passive targeting*". The basis for increased tumor specificity is the differential accumulation of drug-loaded micelles or nanoparticles in tumor tissue versus normal tissues. Passive targeting can therefore result in increased drug concentrations in solid tumors of several-fold relative to those obtained with free drugs.

Target ligands attached to the surface of nanoparticles (Fig. 2) may act as "homing devices", improving the selective delivery of drug to specific tissue and cells (Pirollo and Chang, 2008). Among

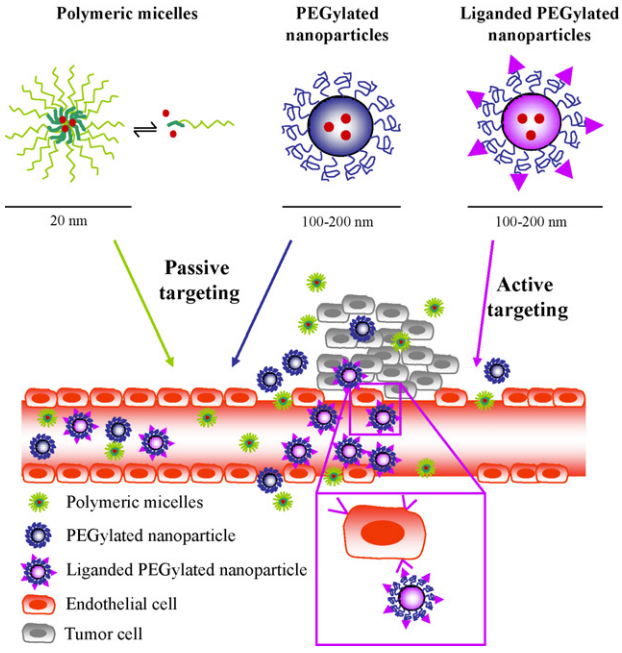

Fig. 2. Schematic representation of polymeric micelles, PEGylated nanoparticles and liganded nanoparticles. The PEGylation allows nanoparticles an extended circulation time, avoiding the opsonization of macrophages. Polymeric micelles and PEGylated nanoparticles reach tumors selectively through the leaky vasculature surrounding the tumors (EPR effect—passive targeting) whereas ligands grafted at the surface of nanoparticles allow active targeting by binding to receptors over-expressed by cancer cells or angiogenic endothelial cells.

various ligands currently developed allowing the "*active targeting*" of tumors, the tripeptide arginine-glycine-aspartic acid (RGD) has been shown to bind preferentially to integrins (in particular $\alpha_v\beta_3$) that are over-expressed in angiogenic endothelial cells. Targeting the $\alpha_v\beta_3$ integrin with drugs may provide an opportunity to target the tumor and to destroy tumor vessels without harmful effects on microvessels of normal tissue (Arap et al., 1998; Byrne et al., 2008).

As nanoencapsulation of poorly soluble CDK1 has never been studied for CDK solubilization and/or tumor targeting, the aims of this work were (i) to solubilize and formulate the novel CDK inhibitor, JNJ-7706621, for the parenteral route; (ii) to compare anti-cancer efficacy of this drug by passive or active targeting using polymeric micelles and nanoparticles; and finally (iii) to study the potential synergy of the JNJ-7706621 compound with PTX.

Therefore JNJ-7706621 was encapsulated in PEG-p-(CL-*co*-TMC) micelles and in PEGylated PLGA-based nanoparticles. Self-assembling diblock copolymers made up of ε-caprolactone (CL) and trimethylene carbonate (TMC) and mmePEG$_{750}$ (mmePEG$_{750}$-p-(CL-*co*-TMC)) have been shown to form micelles spontaneously upon gentle mixing with water. These copolymers are biocompatible, non-cytotoxic and non-hemolytic. They increase the solubility of poorly soluble-water drugs (including PTX) by one to four orders of magnitude (Ould-Ouali et al., 2004; Danhier et al., 2009a). PEGylated PLGA-based nanoparticles loaded with PTX prepared by nanoprecipitation method have been developed (Danhier et al., 2009b). Poly(lactide-co-glycolide) (PLGA) was chosen for its biodegradability properties, its biocompatibility and the fact that related polyesters have been previously approved by the FDA. Poly(ε-caprolactone-co-ethylene glycol) (PCL-PEG), an amphiphilic copolymer, was added to take advantage of PEG steric stabilization properties, to provide a higher stability of nanoparticles in biological fluids and to allow the grafting of RGD peptide on the polymer (Owens and Peppas, 2006; Garinot et al., 2007). RGD-grafted PLGA nanoparticles have been shown to target the $\alpha_v\beta_3$ integrin of the tumor endothelium (Danhier et al., 2009c). The in vitro anti-tumoral activity of JNJ-7706621-loaded micelles and nanoparticles was assessed using Human Cervix Epithelial Carcinoma (HeLa) cells. The apoptosis induced by JNJ-7706621-loaded micelles or nanoparticles was also studied. To compare the passive and active targeting of the anti-cancer drugs to tumors, in vivo anti-tumor efficacy of JNJ-7706621-loaded micelles, nanoparticles and RGD-grafted nanoparticles was investigated in mice bearing a fast growing tumor: the transplantable liver tumors (TLT). Finally, the combination of PTX-loaded micelles (Danhier et al., 2009a) or nanoparticles grafted or not (Danhier et al., 2009b,c) with these JNJ-7706621-loaded micelles or nanoparticles grafted or not was performed in TLT-tumor-bearing mice to evaluate the synergy between these two drugs.

2. Materials and methods

2.1. Materials

PLGA, PCL-b-PEG, PLGA-b-PEG polymers were synthesized by ring opening polymerization. Preparation of PCL-b-PEG grafted with GRGDS was performed as previously described by photografting (Garinot et al., 2007; Pourcelle et al., 2007). Molecular weights were determined by size exclusion chromatography (SEC) and NMR as described previously. The PEG-p(CL-*co*-TMC) diblock copolymers were synthesized by the Johnson and Johnson Advanced Technologies and Regenerative Medecine (ATRM) (Somerville, NJ, USA). Characteristics of polymers are summarized in Table 1. PTX was purchased from Calbiochem (Darmstadt, Germany). Taxol® was obtained from Brystol-Myers Squibb. JNJ-7706621 was provided by Johnson and Johnson, Pharmaceutical Research and Development (Beerse, Belgium).

Table 1
Chemical description of the polymers included in the formulations.

Nanoparticle polymers	Mw (g/mol)[a]	Mn[b] (g/mol)	Mn (NMR)[a] (g/mol)	PDI[c]
PLGA	39,600	22,000	–	1.8
PLGA-FITC	37,800	23,600	–	1.6
PLGA-b-PEG	49,800	29,300	16,500–4,600	1.7
PCL-b-PEG	25,800	22,400	15,200–4,600	1.15
Micelle polymers	**Mw (g/mol)[d]**	**CL/TMC ratio in final polymer[e]**		**PDI[d]**
PEG-p(CL-*co*-TMC)	5,300	49.3 ± 0.4/50.1 ± 0.8		1.9

[a] Determined by NMR by the following formula: $(I_{4.7}/2)/(I_{5.2} + I_{4.7}/2) \times 100$, where $I_{4.7}$ is the signal intensity of the glycolide unit at 4.7 ppm ($CH_2OC{=}O$) and $I_{5.2}$ is the signal intensity of the lactide unit at 5.2 ppm ($CH(CH_3)OC{=}O$).
[b] Polystyrene calibration.
[c] PDI = Mw/Mn, determined by SEC by polystyrene standard.
[d] The molecular weight and the polydispersity of the diblock polymer were determined by gel permeation chromatography and the monomer ratio in the polymer by NMR spectroscopy.
[e] The monomer composition was evaluated by NMR.

HeLa (Human Cervical Carcinoma) cells were acquired from ATCC (American Type Culture Collection, Manassas, VA, USA). 4,6-Diamidino-2-phenylindole (DAPI) and 3-(4,5-dimethylthiazol-2-yl)-2,5-diphenyl tetrazolium bromide (MTT) were purchased from Sigma–Aldrich (St. Louis, MO, USA). Dubelcco's modified Eagle's medium (DMEM), fetal bovine serum, trypsin–EDTA and penicillin–streptomycin mixtures were from Gibco® BRL (Carlsbad, CA, USA). Ultra-purified water was used throughout and all other chemicals were of analytical grade.

NMRI mice were purchased from Janvier, Genest-St-Isle, France. The transplantable liver tumors TLT (syngeneic tumors) were obtained from UCL (Brussels, Belgium) (Taper et al., 1966).

2.2. Formulations of polymeric micelles and nanoparticles loaded with JNJ-7706621 and PTX

The solubility of JNJ-7706621 in 10% (w/v) PEG-p(CL-*co*-TMC) in water was determined. JNJ-7706621 was added to PEG-p(CL-*co*-TMC) and mixed overnight at 37 °C. Ultra-pure water was then added drop-wise to form the micellar solution. The excess drug was removed by filtration through 0.45 μm PVDF filters. PTX-loaded micelles were similarly prepared as previously described (Danhier et al., 2009a).

Nanoparticles were prepared by the interfacial deposition method (nanoprecipitation) (Danhier et al., 2009b,c). Briefly, an organic solution of PLGA (70 mg), PLGA-b-PEG (15 mg), PCL-b-PEG or PCL-b-PEG-g-GRGDS (15 mg) and JNJ-7706621 (5 mg) or PTX (1 mg) in 10 ml acetone was added to 20 ml water under magnetic stirring at room temperature overnight to allow the evaporation of acetone. To remove the non-encapsulated drug, the suspensions were filtered (1.2 μm) and ultracentrifuged at 22,000 × *g* for 1 h at 4 °C. The pellets were suspended in adequate volume of ultra-purified water. A suspension of JNJ-7706621, used as the control, was obtained by dispersing 6.5 mg of the drug in 10 ml of a 1.25% Pluronic® F108 solution.

2.3. Physicochemical characterization of JNJ-7706621-loaded micelles and nanoparticles

The amount of JNJ-7706621 solubilized in micelles or entrapped in nanoparticles was determined in triplicate by HPLC (Agilent 1100 series, Agilent Technologies, Diegem, BE). The samples were eluted with a linear gradient of 0.2% ammonium acetate in water (A) and acetonitrile (B), from 100% (0 min) to 20% (12 min). A reverse phase column CC 125/4 Nucleodur 100-5 C18 (Macherey–Nagel, Germany) was maintained at 30 °C. The flow rate was set at 1.2 ml/min and the detection wavelength was 272 nm. Sample solution was injected at a volume of 10 μl. The HPLC was calibrated with solutions of 1–200 μg/ml of JNJ-7706621 dissolved in acetonitrile and citrate–phosphate buffer pH 7 (correlation coefficient of $R^2 = 0.99$, LOD = 0.5 μg/ml, LOQ = 1 μg/ml, coefficients of variation < 5.2%). Micelles were diluted in acetonitrile. Nanoparticles were dissolved in acetonitrile and vigorously vortexed to get a clear solution. The encapsulation efficiency was defined by the ratio of measured JNJ-7706621 encapsulated in nanoparticles and initial amount of the drug.

$$\text{encapsulation efficiency (\%)} = \frac{\text{amount of JNJ-7706621 in nanoparticles}}{\text{initial amount of JNJ-7706621}} \times 100$$

The particle size and ζ potential of both JNJ-7706621-loaded micelles and nanoparticles were determined, respectively, by photon correlation spectroscopy (PCS) and laser Doppler velocimetry using a Zetasizer® Nano ZS (Malvern Instruments, UK). The measurements were performed in triplicate in PBS (phosphate buffered solution, pH 7.4) (Danhier et al., 2009b). The primary volume median particle diameter of the suspension of JNJ-7706621 was measured by laser diffraction (HELOS, Sympatec, Clausthal-Zellerfeld, Germany). The suspension was suspended in water in a 50 ml glass cuvette and stirred with a magnetic bar at 1000 rpm. A short period of sonication (30–60 s) at a power of 60 W (CUVETTE, Sympatec) was applied before sizing.

2.4. In vitro anti-tumoral activity

2.4.1. Evaluation of anti-tumoral activity of JNJ-770662-loaded micelles and nanoparticles

HeLa cells were grown in DMEM supplemented with 10% (v/v) fetal bovine serum, 100 IU/ml of penicillin G sodium and 100 μg/ml of streptomycin sulfate. The cells were maintained in an incubator supplied with 5% CO_2/95% humidified atmosphere at 37 °C.

HeLa cells were seeded in 96-well plates at the density of 2500 viable cells per well. The cells were then incubated with a suspension of JNJ-7706621, JNJ-7706621-loaded micelles and nanoparticles (JNJ-7706621 concentrations of 0.011, 0.022, 0.11, 0.22, 1.1, 2.2, 11 and 22 μg/ml; dilutions were made in the medium) and drug-free polymeric micelles (polymers concentrations 0.3 mg/ml) and nanoparticles (polymers concentration 5 mg/ml) for 4, 24 and 48 h. The cytotoxicity was assessed using the MTT test as previously described (Mosmann, 1983; Danhier et al., 2009b). Absorbance was measured at 570 nm using a microplate reader (Thermo Scientific, USA). Untreated cells were taken as control with 100% viability and Triton X-100 1% was used as positive control of cytotoxicity. The results were expressed as mean values ± standard deviations of five measurements.

Table 2
Time schedule of combined treatments.

Mice Groups	Day 0	Days 1–5
1. PBS (control)	PBS	PBS
2. Taxol-JNJ suspension	Taxol®[a]	JNJ suspension[b]
3. PTX-JNJ micelles	PTX-loaded micelles[a]	JNJ-loaded micelles[a]
4. PTX-JNJ nanoparticles	PTX-loaded nanoparticles[a]	JNJ-loaded nanoparticles[a]
5. PTX-JNJ nanoparticles RGD	PTX-loaded nanoparticles RGD[a]	JNJ-loaded nanoparticles RGD[a]

[a] Intravenous injection.
[b] Intraperitoneal injection.

2.4.2. Measure of apoptosis

Apoptosis was identified morphologically by 4,6-diamidino-2-phenylindole (DAPI) staining. As previously described (Danhier et al., 2009b), HeLa cells were seeded in 6-well plates containing a cover slip with 10^5 cells per well and incubated for 8 h with JNJ-7706621-loaded micelles and nanoparticles (JNJ-7706621 concentration of 22 μg/ml) and culture medium as control. Samples were fixed with 4% paraformaldehyde in PBS and then stained with 0.2 μg/ml DAPI in PBS. Cover slips were examined using a fluorescent microscope (Zeiss, Wetzlar, Germany) with a 340/380 nm excitation filter and LP 430 nm barrier filter. Enumeration of apoptotic nuclei was made on slides picked up at random by two independent observers. Clusters of apoptotic bodies were given as a single count.

2.5. Effect of JNJ-7706621-loaded micelles and nanoparticles on tumor growth

2.5.1. Animal tumor model

The transplantable liver tumors TLT (syngeneic tumors) were implanted in the gastrocnemius muscle in the posterior leg of 8-week-old male NMRI mice. These hepatocarcinoma cells were chosen because it has been demonstrated previously that this model is sensible to chemotherapy (Jordan et al., 2003; Danhier et al., 2009a,b,c).

All experiments were approved by the ethical committee for animal care of the faculty of medicine of the Université Catholique de Louvain. The effect of treatments on TLT growth was assessed. When tumors reached 8.0 ± 0.5 mm in diameter, the mice were randomly assigned to a treatment group. After treatment, tumors were measured every day until they reached a diameter of 18 mm, at which time the mice were sacrificed. Changes in body weight were also monitored.

2.5.2. Treatments with PTX and JNJ-7706621-loaded micelles and nanoparticles

Five groups of mice (six mice per group) were treated—group 1: PBS injection; group 2: a suspension of JNJ-7706621; group 3: JNJ-7706621-loaded micelles; group 4: JNJ-7706621-loaded nanoparticles; group 5: JNJ-7706621-loaded RGD-nanoparticles. Except for the JNJ-7706621 suspension, injected intraperitonealy, all the treatments were injected through the tail vein of mice each day for 5 days. All formulations of JNJ-7706621 were daily administered at the dose of 3.25 mg/kg.

The combination of PTX and JNJ-7706621 was also investigated. Time schedule of combined treatments is summarized in Table 2. Both PTX and JNJ-7706621 were injected intravenously in drug-loaded micelles, drug-loaded nanoparticles or drug-loaded nanoparticles grafted with the RGD peptide. Mice received PTX-loaded micelles or nanoparticles at day 0 (PTX dose of 1.35 mg/kg). 24 h post-chemotherapy treatment, mice received JNJ-7706621 micelles or nanoparticles each day for 5 consecutive days (JNJ-7706621 dose of 3.25 mg/kg/day). Controls consisted of PBS injection, injection of Taxol® at day 0 and daily intraperitoneal injections of a suspension of JNJ-7706621 for 5 consecutive days.

2.6. Statistics

All results are expressed as mean ± standard deviation except for Figs. 5 and 6 where results are expressed as mean ± standard error of the mean (SEM). Two-way ANOVA and Bonferroni post test, IC_{50} values (calculated from a dose–response graph (not shown) with sigmoidal function with variable Hill slope) and the Kaplan–Meier survival rate and the median survivals were performed using the software GraphPad Prism 5 for Windows (v 5.00, La Jolla, CA, USA) to demonstrate statistical differences ($p < 0.05$).

3. Results

3.1. Preparation and physicochemical characterization of JNJ-7706621-loaded micelles and nanoparticles

To solubilize the JNJ-7706621 compound, both polymeric micelles and nanoparticles were formulated. Physicochemical characteristics of JNJ-7706621-loaded micelles and nanoparticles are illustrated in Table 3. PEG-p(CL-*co*-TMC) block copolymers, in which the drug was dissolved, form micelles spontaneously upon dilution in aqueous medium. In 10% PEG-p(CL-*co*-TMC) in water, the solubility of JNJ-7706621 increased from 0.017 mg/ml in water to 6.7 ± 0.3 mg/ml. Consistent with previous data (Danhier et al., 2009a), the size and ζ potential of micelles containing 10% PEG-p(CL-*co*-TMC) were 23.3 ± 0.4 nm (PDI: 0.06) and 0.48 ± 2 mV,

Table 3
Physicochemical characterization of JNJ-7706621-loaded micelles and nanoparticles.

	Micelles	Nanoparticles	RGD-nanoparticles
JNJ-7706621 encapsulation efficiency (%)	NA	65 ± 3	63 ± 4
JNJ-7706621 solubility in 10% of PEG-p(CL-*co*-TMC) (mg/ml)	6.7 ± 0.3	NA	NA
JNJ-7706621/polymers (%)	6.7	3.25	3.15
Size (nm)[a]	23.3 ± 0.4	121.7 ± 6	125.9 ± 4
PDI[a]	0.06 ± 0.002	0.17 ± 0.005	0.12 ± 0.003
ζ potential (mV)[b]	0.48 ± 2	0.02 ± 2.7	0.03 ± 2.4
ζ deviation (mV)[b]	4.15 ± 0.98	5.5 ± 1.2	4.6 ± 0.86

Each data represents the mean ± standard deviation ($n = 3$). NA, not applicable.
[a] Measured by photon correlation spectroscopy with a Malvern Nano ZS.
[b] Determined with a Malvern Nano ZS.

respectively. The solubilization of JNJ-7706621 into micelles did not influence the size or the ζ potential of micelles (data not shown).

Nanoparticles prepared by the nanoprecipitation method allowed the encapsulation of 65% of the initial dose of JNJ-7706621. The size and the ζ potential of JNJ-7706621-loaded nanoparticles were 121.7 ± 6 nm (PDI: 0.17) and 0.02 ± 2.7 mV, respectively. Nanoparticles exhibited a neutral ζ potential, confirming the presence of PEG chains shielding the negative charges present at the nanoparticles surface. Previously, we have shown that PEGylated PLGA-based nanoparticles produced by nanoprecipitation presented 41% of PEG exposed at the nanoparticles surface (des Rieux et al., 2007). Replacement of PCL-PEG in the formulation by PCL-PEG-g-GRGDS did not modify the encapsulation efficiency, the size and the ζ potential of the particles, as reported previously (Danhier et al., 2009c). The presence of RGD at the surface of nanoparticles was confirmed by XPS (Pourcelle et al., 2007).

The physicochemical characterization of PTX-loaded micelles and nanoparticles was described previously (Danhier et al., 2009a,b,c). Briefly, PEG-p(CL-*co*-TMC) increased the aqueous solubility of PTX by three orders of magnitude. The size and ζ potential of PTX-loaded micelles containing 10% PEG-p(CL-*co*-TMC) were 23.4 ± 0.3 nm and -2.9 ± 0.3 mV, respectively (Danhier et al., 2009a). The encapsulation efficiency of PTX-loaded nanoparticles and RGD-nanoparticles was 70 and 61%, respectively. The size of PTX-loaded nanoparticles was 114 nm, while the size of PTX-loaded RGD-nanoparticles was slightly larger (138 nm). The two formulations exhibited a ζ potential close to 0 mV (Danhier et al., 2009b,c). The particles size of the JNJ-7706621 suspension was 56.1 ± 4.1 μm.

3.2. *In vitro anti-tumoral activity of JNJ-7706621-loaded micelles and nanoparticles*

To check if the loading in micelles or nanoparticles affected cell growth and cell apoptosis, in vitro anti-tumoral activity of JNJ-7706621-loaded micelles and nanoparticles was investigated on HeLa cells. Cell viability was measured using the MTT assay after 4, 24 and 48 h treatment by a suspension of JNJ-7706621, JNJ-7706621-loaded micelles and nanoparticles (Fig. 3). Concentrations of the drug tested ranged from 0.011 to 22 μg/ml.

Table 4
IC_{50} of JNJ-7706621 suspension and JNJ-7706621-loaded nanoparticles or micelles.

	IC_{50} at 24 h (μg/ml)	IC_{50} at 48 h (μg/ml)
JNJ-7706621 suspension	2.1	0.9
JNJ-7706621 nanoparticles	35	2.7
JNJ-7706621 micelles	6.3	1.6

After 4 h, the cell viability was more inhibited by the suspension of JNJ-7706621 than by JNJ-7706621-loaded micelles or nanoparticles at the concentrations of JNJ-7706621 of 22 and 2.2 μg/ml ($p < 0.001$ and $p < 0.05$, respectively). For lower concentrations, no significant difference was observed ($p > 0.05$) (Fig. 3A). After 24 and 48 h, an influence of the concentrations of JNJ-7706621 on cell viability could be observed (Fig. 3B and C). The higher the concentrations, the lower the cell viability. The IC_{50} at 24 and 48 h of the JNJ-7706621 suspensions were 2.1 and 0.9 μg/ml; the IC_{50} of the JNJ-7706621-loaded nanoparticles were 35 and 2.7 μg/ml and the IC_{50} of the JNJ-7706621-loaded micelles were 6.3 and 1.6 μg/ml (Table 4). At the concentrations used, Pluronic® F108, PEG-p(CL-*co*-TMC) and PLGA-based PEGylated nanoparticles did not induce any cytotoxicity (data not shown).

The induction of apoptosis of JNJ-7706621 was confirmed by DAPI staining of the nuclei (Fig. 4). The nuclei of untreated HeLa cells showed homogenous fluorescence with no evidence of segmentation on fragmentation while nuclei of cells treated for 8 h by JNJ-7706621-loaded micelles or nanoparticles were fragmented, indicative of apoptosis. The percentage of apoptotic cells induced by JNJ-7706621-loaded micelles ($34.6 \pm 6.6\%$) and nanoparticles ($25 \pm 4.8\%$) was not significantly different ($p > 0.05$). Similar results were observed for other drug concentrations and incubation time (data not shown).

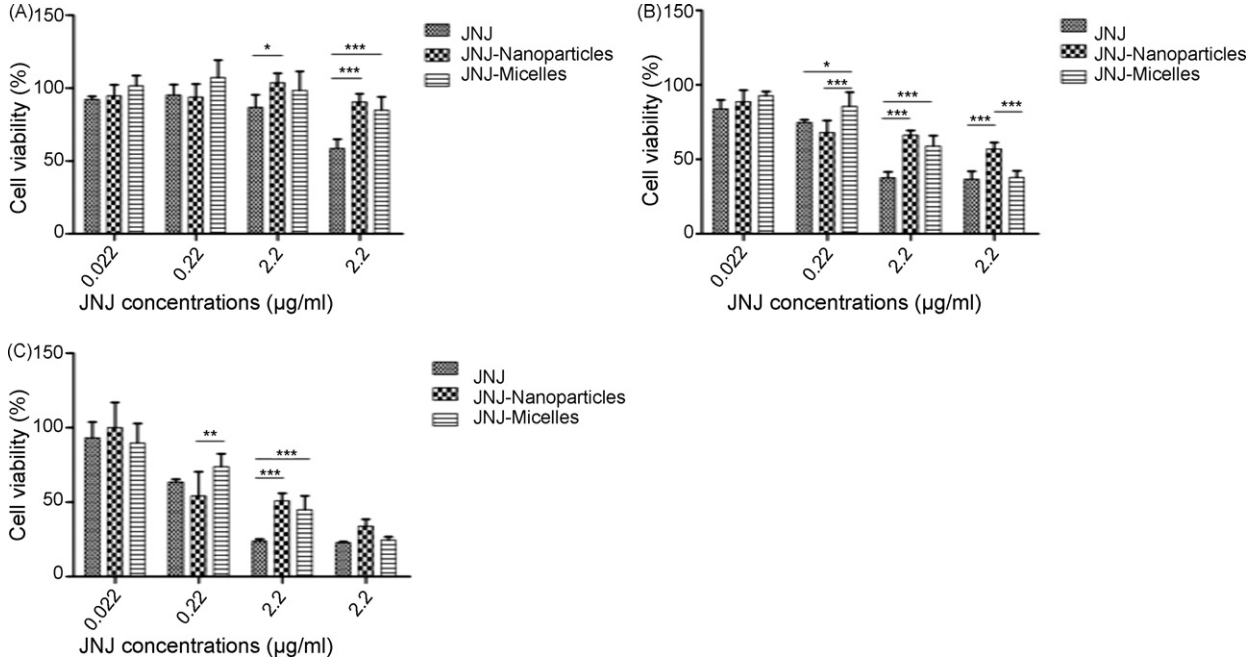

Fig. 3. Viability of HeLa cells incubated with a suspension of JNJ-7706621, JNJ-7706621-loaded micelles and nanoparticles (JNJ-7706621 concentrations 0.011–22 μg/ml) after 4 h (A), 24 h (B) and 48 h (C). Cell viability was determined by the MTT assay. Untreated cells were taken as negative control and Triton X-100 1% was used as positive control. The results were expressed as mean values ± standard deviation ($n = 5$). $^{*}p < 0.05$; $^{**}p < 0.01$; $^{***}p < 0.001$.

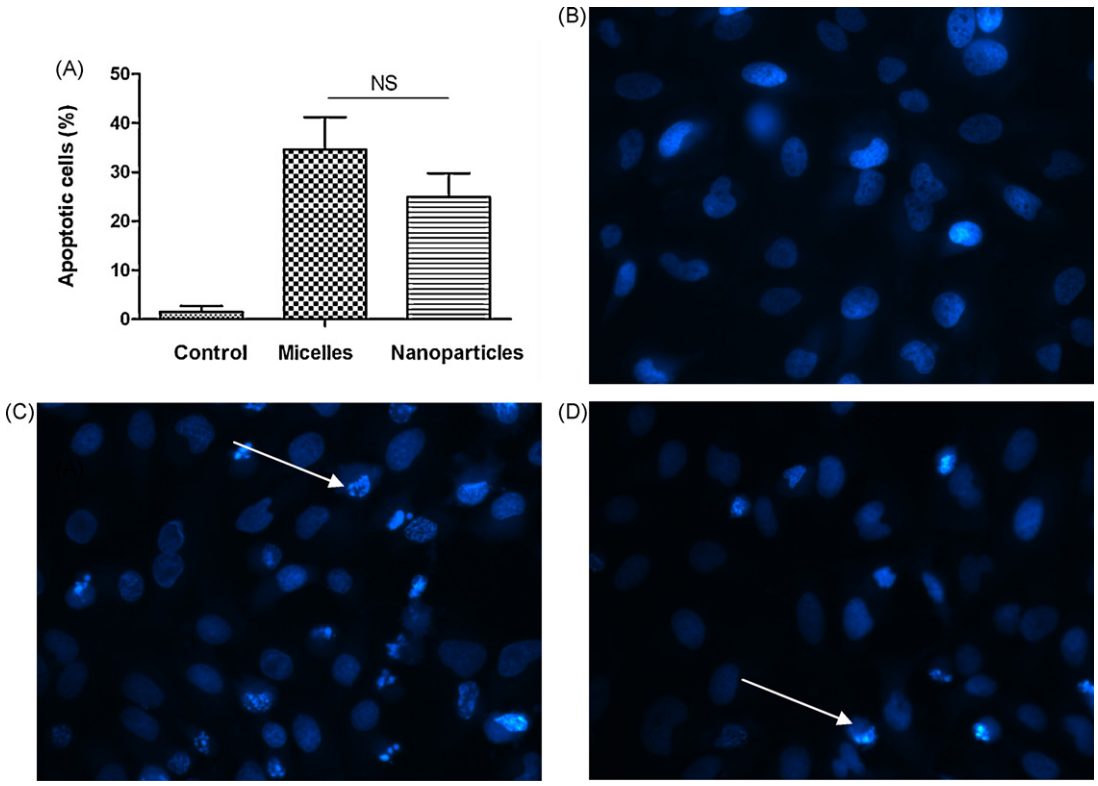

Fig. 4. DAPI staining of HeLa cells after incubation for 8 h of culture medium as control, JNJ-7706621-loaded micelles and nanoparticles (JNJ-7706621 concentration 22 μg/ml) ($n = 3$). (A) Percentage of apoptotic cells (DAPI staining). Enumeration of apoptotic nuclei (about 200 cells were counted) was made on slides picked up at random by two independent experimenters. Clusters of apoptotic bodies were given as a single count. The results were expressed as mean values ± standard deviation. (B) Untreated cells as control. (C) Cells treated by JNJ-7706621-loaded micelles. (D) Cells treated by JNJ-7706621-loaded nanoparticles.

3.3. Effect of JNJ-7706621-loaded micelles and nanoparticles on tumor growth

To compare the efficacy of passive targeting (micelles and nanoparticles) and active targeting (RGD-grafted nanoparticles), the in vivo anti-tumor efficacy of JNJ-7706621-loaded micelles, nanoparticles and RGD-nanoparticles was evaluated in TLT-tumor-bearing mice (Fig. 5). All treatments were statistically different compared to the PBS control ($p < 0.001$). The three JNJ-7706621-loaded nanocarriers delayed the tumor growth more efficiently than the control JNJ-7706621 suspension (Fig. 5A).

The survival rate (corresponding to the sacrifice of mice when tumors reached 18 mm) was significantly higher for mice treated with JNJ-7706621-loaded micelles, nanoparticles and RGD-nanoparticles as compared to the drug suspension ($p < 0.05$; $p < 0.01$; $p < 0.001$, respectively). The median survivals were 13.8 days for JNJ-7706621-loaded micelles, 15.3 days for nanoparticles, 16.8 days for RGD-nanoparticles and 9.8 days for the drug suspension. No difference was observed for mice treated by JNJ-7706621-loaded micelles and nanoparticles ($p > 0.05$), while JNJ-7706621-loaded RGD-nanoparticles exhibited a higher survival rate than JNJ-7706621-loaded micelles or nanoparticles ($p < 0.05$) (Fig. 5B).

As CDK inhibitors efficacy has been reported to be enhanced by apoptosis-inducing anti-cancer drugs (Sedlacek, 2001), we evaluated the potential synergy of these JNJ-7706621 formulations

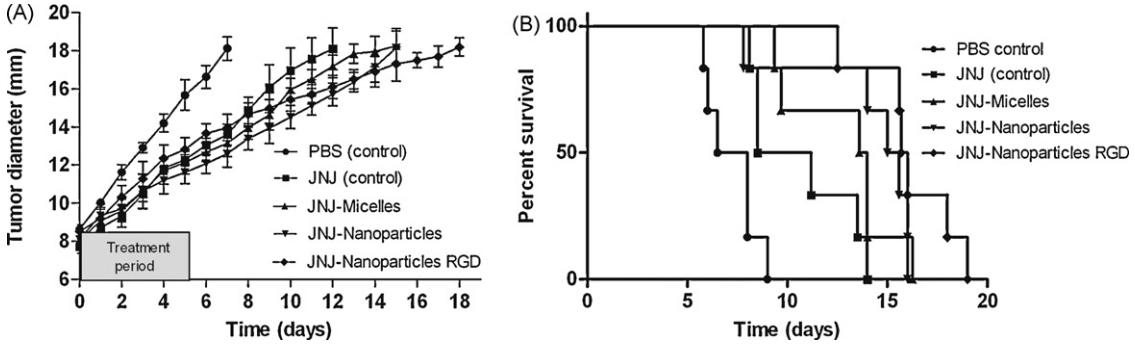

Fig. 5. Anti-tumor effect on TLT-tumor-bearing mice treated with JNJ-7706621-loaded micelles, nanoparticles and RGD-nanoparticles alone (JNJ-7706621 dose of 3.25 mg/kg/day). Controls of JNJ-7706621 consisted in a suspension of the drug candidate in Pluronic® F108. (A) Anti-tumor effect of a suspension of JNJ-7706621, JNJ-7706621-loaded micelles, nanoparticles and RGD-nanoparticles on TLT-tumor-bearing mice. JNJ-7706621 (3.25 mg/kg/day) treatments were injected intravenously (intraperitonealy for the suspension) each day for 5 days. Five groups of mice were treated—group 1: PBS injection; group 2: a suspension of JNJ-7706621; group 3: JNJ-7706621-loaded micelles; group 4: JNJ-7706621-loaded nanoparticles; group 5: JNJ-7706621-loaded RGD-nanoparticles. Each point represents the mean of tumor size ± SEM ($n = 6$). (B) Survival rates of tumor-bearing mice.

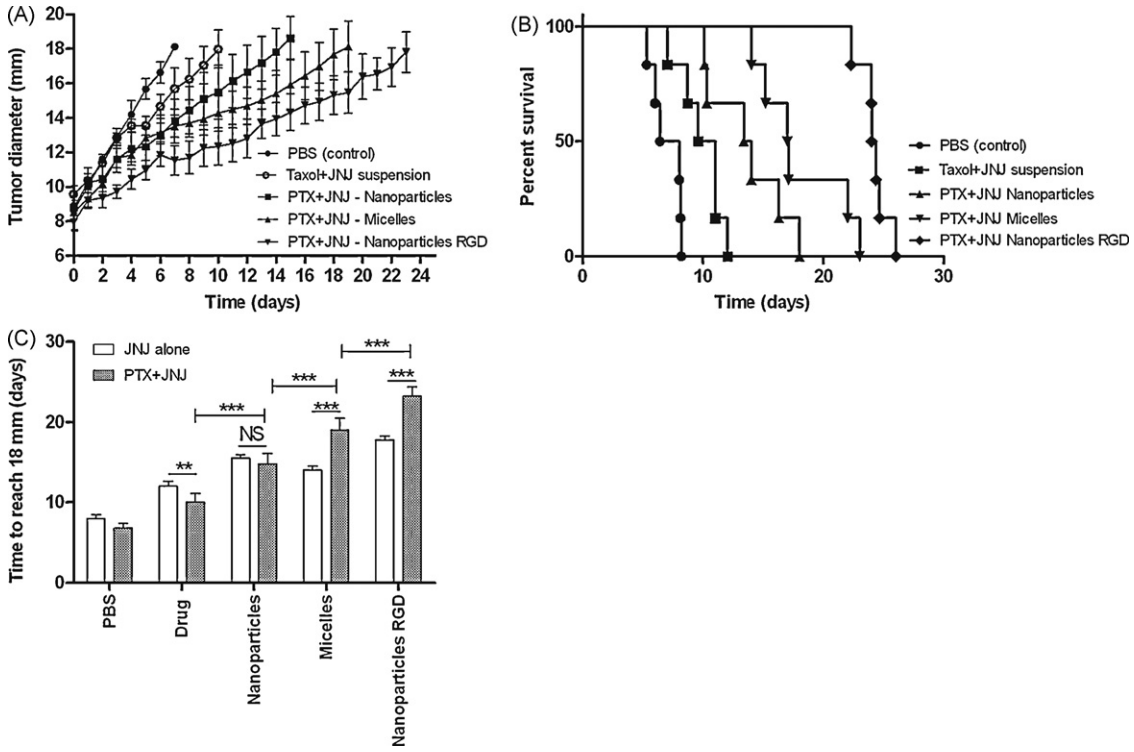

Fig. 6. Anti-tumor effect on TLT-tumor-bearing mice treated with the combination of PTX and JNJ-7706621-loaded micelles, nanoparticles and RGD-nanoparticles (JNJ-7706621 dose of 3.25 mg/kg/day; PTX dose of 1.35 mg/kg). Controls of JNJ-7706621 and PTX consisted in a suspension of JNJ-7706621 in Pluronic® and Taxol®, respectively. (A) Anti-tumor effect of the combination of PTX and JNJ-7706621 encapsulated into micelles, nanoparticles and RGD-nanoparticles. Mice received PTX-loaded micelles or nanoparticles at day 0. 24 h post-chemotherapy treatment, mice received JNJ-7706621 micelles or nanoparticles each day for 5 days. Each point represents the mean of tumor size ± SEM ($n = 6$). (B) Survival rates of tumor-bearing mice. (C) Comparison of time for TLT tumor to reach 18 mm of JNJ-7706621 treatments alone and the combination of PTX and JNJ-7706621 treatments. $^{**}p < 0.01$; $^{***}p < 0.001$.

with PTX-loaded micelles, nanoparticles and RGD-nanoparticles previously developed in our laboratory (Danhier et al., 2009a,b,c) (Table 2). The combination of PTX and JNJ-7706621-loaded micelles and nanoparticles inhibited tumor growth more efficiently than the combination of Taxol® and the JNJ-7706621 suspension (Fig. 6A).

For mice treated with PTX- and JNJ-7706621-loaded micelles, nanoparticles and RGD-nanoparticles, the survival rate was higher than for the combination of Taxol® and JNJ-7706621 suspension ($p < 0.001$; $p < 0.05$; $p < 0.001$). The median survivals were 17 days for JNJ-7706621-loaded micelles, 13.7 days for nanoparticles, 24.2 days for RGD-nanoparticles and 10.3 days for the dug suspension. The survival rate was higher for the combination of PTX and JNJ-7706621-loaded micelles than for the combination of PTX and JNJ-7706621-loaded nanoparticles ($p < 0.05$). The combination of PTX and JNJ-7706621-loaded RGD-nanoparticles exhibited a higher survival rate than the combination of PTX and JNJ-7706621-loaded micelles or nanoparticles ($p < 0.01$; $p < 0.001$, respectively) (Fig. 6B).

The benefits of the combination of PTX with JNJ-7706621 encapsulated into polymeric micelles or nanoparticles grafted with or without the RGD peptide are illustrated in Fig. 6C. The time to reach 18 mm was equivalent for mice treated with JNJ-7706621-loaded nanoparticles and the combination of PTX and JNJ-7706621-loaded nanoparticles ($p > 0.05$). The administration of PTX and JNJ-7706621-loaded micelles prolonged the time to reach 18 mm tumor diameter when compared to JNJ-7706621-loaded micelles alone (19 and 15 days, respectively) ($p < 0.001$). For mice treated by the combination of PTX and JNJ-7706621-loaded RGD-nanoparticles, the time to reach 18 mm was also longer than for JNJ-7706621-loaded RGD-nanoparticles alone (23 and 18 days, respectively) ($p < 0.001$).

Body weight measurements showed no significant differences between the groups throughout the study. There was a slight increase in body mass as a result of natural animal growth (data not shown).

4. Discussion

The aims of this work were (i) to formulate the poorly soluble anti-cancer drug JNJ-7706621 intended to be injected intravenously, (ii) to compare the effect of passive and active targeting of this drug on tumor growth and (iii) to evaluate the potential synergy of JNJ-7706621 with PTX. Hence, we used two nanotechnologies: polymeric micelles and nanoparticles. These drug delivery systems can accumulate in tumors by the enhanced permeation and retention (EPR) effect, which can be considered as a form of "passive targeting" to the tumors. Target ligands (e.g. the tripeptide RGD) can be attached to the surface of nanoparticles allowing for the "active targeting" of tumors.

To our knowledge, no previous report describes encapsulation of CDK inhibitors in nanocarriers. We demonstrated that JNJ-7706621 can be efficiently encapsulated in self-assembling polymeric micelles and in PEGylated PLGA-based nanoparticles. These nanocarriers, with a size of 25 and 125 nm, respectively, can be intravenously injected and can deliver therapeutic doses of JNJ-7706621. The stability of these systems has been previously shown: blood concentrations of PEG-p(CL-*co*-TMC) remained at least 48 h above the critical micellar concentration (CMC) (Danhier et al., 2009a); while PEGylated nanoparticles are known to avoid opsonization of macrophages (Owens and Peppas, 2006).

In vitro, the JNJ-7706621 control suspension showed a higher anti-tumoral activity compared to the JNJ-7706621 entrapped into micelles and nanoparticles after 24 and 48 h, probably because the free drug in the medium is higher in a suspension. At the concentrations tested, Pluronic® F108, PEG-p(CL-*co*-TMC) and PLGA-based

PEGylated nanoparticles did not induce cytotoxicity (Wong et al., 2008; Danhier et al., 2009a,b). The differences of IC_{50} of JNJ-7706621-loaded nanoparticles or micelles when compared to the JNJ-7706621 control suspensions could be explained by differences in the internalization of the drug when formulated as a nanoparticulate system or a suspension. Generally, nanoparticles are non-specifically internalized into cells via endocytosis or phagocytosis (des Rieux et al., 2006; Breunig et al., 2008). The internalization of micelles proceeds via endocytosis (Rapoport, 2008) and unimers of PEG-p(CL-*co*-TMC) passively diffuse across enterocytes while PEG-p(CL-co-TMC) micelles utilized fluid phase pinocytosis (Mathot et al., 2007). The decrease in cell viability induced by JNJ-7706621, measured by the MTT test could result from an inhibition of cell growth or from cytotoxicity.

Selective inhibition of CDK limits the progression of a tumor cell through the cell cycle and facilitates the induction of apoptotic pathways (Lapenna and Giordano, 2009). It has been shown that cells exposed to JNJ-7706621 arrest in G_2/M, inducing apoptosis, depending on drug concentration and length of exposure (Emanuel et al., 2005). As expected, JNJ-7706621 entrapped into polymeric micelles or nanoparticles was able to induce apoptosis of tumor cells.

In vivo, JNJ-7706621-loaded micelles, nanoparticles and RGD-grafted nanoparticles induced a significant delay in tumor growth as compared to the JNJ-7706621 control suspension. JNJ-7706621 was administered for 5 consecutive days, similarly with flavopiridol treatments described in the literature (Mason et al., 2004). For the fist time, different nanotechnologies were studied in one experiment, allowing the comparison of drug delivery by passive and active targeting. Due to their ability to actively target the tumors and to enhance drug delivery to tumors (Danhier et al., 2009c), JNJ-7706621-loaded RGD-nanoparticles had a greater effect on the delay of tumor growth than did other JNJ-7706621 formulations. For mice treated with JNJ-7706621-loaded micelles and nanoparticles, which target the tumors passively, no significant difference was observed. Micelles or nanoparticles induced a significant delay in tumor growth but were unable to provide tumor regression due to the intrinsic resistance and fast growth of the TLT model. We have shown previously that PEG-p(CL-*co*-TMC) micelles are associated with low blood clearance, a relatively weak capture by the RES and that they accumulate by the EPR effect in tumors (Danhier et al., 2009a). In vitro and in vivo studies on human umbilical vein endothelial cells (HUVEC) clearly demonstrated the active targeting of our PEGylated PLGA-based nanoparticles grafted with the RGD peptide to tumor endothelium via $\alpha_v\beta_3$ integrins (Danhier et al., 2009c). Hence for JNJ-7706621-loaded RGD-nanoparticles, the combined effect of passive accumulating and specific tumor targeting should be responsible for the improved therapeutic efficacy. Moreover, the tumor targeting ability of JNJ-7706621-loaded RGD-nanoparticles could reduce in vivo toxicity in normal tissue.

Combination of CDK inhibitors, such as flavopiridol, and cytostatics, particularly PTX, is described in the literature (Shah and Schwartz, 2003). Based on published treatment schedules, we chose to dose mice with PTX 24 h before the CDK inhibitor administration. The rationale for this sequence of PTX followed by flavopiridol dosing is associated with increased apoptosis and accelerated exit of cells from mitosis (Bible and Kaufmann, 1997). The synergy of this combination has been demonstrated in a clinical Phase II evaluation (Schwartz et al., 2001). The synergy between PTX and JNJ-7706621 was also demonstrated. The prolonged growth delay allows one to discriminate the efficacy between micelles and nanoparticles (passive targeting). The combination of PTX and JNJ-7706621-loaded micelles delayed the tumor growth to a greater extent than did nanoparticles. A possible explanation for this may be related to the smaller size of micelles allowing a better passage through fenestrations in the tumor endothelium. The enhanced tumor targeting of RGD-nanoparticles was even more marked, confirming that active targeting the anti-cancer drugs to the tumor endothelium can enhance their efficacy.

5. Conclusion

JNJ-7706621, a novel poorly soluble anti-cancer drug with cyclin dependent kinase inhibiting properties, was encapsulated in polymeric micelles and nanoparticles for solubilization and tumor targeting purposes. The IC_{50} of JNJ-7706621-loaded micelles and nanoparticles decreased after 48 h; this decrease in cell viability was associated with induction of apoptosis. TLT-tumor-bearing mice treated with JNJ-7706621-loaded micelles, nanoparticles and RGD-grafted nanoparticles decreased tumor growth as compared to the control suspension. The combination of PTX with JNJ-7706621 was more effective than either treatment. Passive targeting of micelles was more effective than passive targeting of nanoparticles. The greatest delay in tumor growth was obtained with the combination of PTX and JNJ-7706621-loaded RGD-nanoparticles which actively target the tumor endothelium. Therefore, active targeting of JNJ-7706621-loaded nanocarriers may be considered an effective anti-cancer drug delivery system for CDK1 inhibitor, particularly in combination with PTX.

Acknowledgments

The authors wish to thank Johnson & Johnson, Pharmaceutical Research and Development, Division of Janssen Pharmaceutica, Belgium for providing Paclitaxel and JNJ-7706621. This work was supported by the FRSM (Belgium). The authors thank Pr. C. Jérôme and H. Freichels for providing PLGA-b-PEG and PCL-b-PEG and Pr. J. Marchand-Brynaert and V. Pourcelle for grafting RGD peptide on PCL-b-PEG.

References

Arap, W., Pasqualini, R., Ruoslahti, E., 1998. Cancer treatment by targeted drug delivery to tumor vasculature in a mouse model. Science 279, 377–380.

Bible, K.C., Kaufmann, S.H., 1997. Cytotoxic synergy between flavopiridol (NSC 649890, L86-8275) and various antineoplastic agents: the importance of sequence of administration. Cancer Res. 57, 3375–3380.

Breunig, M., Bauer, S., Goepferich, A., 2008. Polymers and nanoparticles: intelligent tools for intracellular targeting? Eur. J. Pharm. Biopharm. 68, 112–128.

Byrne, J.D., Betancourt, T., Brannon-Peppas, L., 2008. Active targeting schemes for nanoparticle systems in cancer therapeutics. Adv. Drug Deliv. Rev. 60, 1615–1626.

Danhier, F., Magotteaux, N., Ucakar, B., Lecouturier, N., Brewster, M., Préat, V., 2009a. Novel self-assembling PEG-p-(CL-co-TMC) polymeric micelles as safe and effective delivery system for Paclitaxel. Eur. J. Pharm. Biopharm. 73, 230–238.

Danhier, F., Lecouturier, N., Vroman, B., Jérôme, C., Marchand-Brynaert, J., Feron, O., Préat, V., 2009b. Paclitaxel-loaded PEGylated PLGA-based nanoparticles: in vitro and in vivo evaluation. J. Control. Release 133, 11–17.

Danhier, F., Vroman, B., Lecouturier, N., Crokart, N., Pourcelle, V., Freichels, H., Jerome, C., Marchand-Brynaert, J., Feron, O., Préat, V., 2009c. Targeting of tumor endothelium by RGD-grafted PLGA-nanoparticles loaded with Paclitaxel. J. Control. Release 140, 166–173.

des Rieux, A., Fievez, V., Garinot, M., Schneider, Y.J., Préat, V., 2006. Nanoparticles as potential oral delivery systems of proteins and vaccines: a mechanistic approach. J. Control. Release 116, 1–27.

des Rieux, A., Fievez, V., Momtaz, M., Detrembleur, C., Alonso-Sande, M., Van Gelder, J., Cauvin, A., Schneider, Y.J., Préat, V., 2007. Helodermin-loaded nanoparticles: characterization and transport across an in vitro model of the follicle-associated epithelium. J. Control. Release 118, 294–302.

Emanuel, S., Rugg, C.A., Gruninger, R.H., Lin, R., Fuentes-Pesquera, A., Connolly, P.J., Wetter, S.K., Hollister, B., Kruger, W.W., Napier, C., Jolliffe, L., Middleton, S.A., 2005. The in vitro and in vivo effects of JNJ-7706621: a dual inhibitor of cyclin-dependent kinases and aurora kinases. Cancer Res. 65, 9038–9046.

Garinot, M., Fievez, V., Pourcelle, V., Stoffelbach, F., des, Rieux.A., Plapied, L., Theate, I., Freichels, H., Jérôme, C., Marchand-Brynaert, J., Schneider, Y.J., Préat, V., 2007. PEGylated PLGA-based nanoparticles targeting M cells for oral vaccination. J. Control. Release 120, 195–204.

Jordan, B.F., Sonveaux, P., Feron, O., Grégoire, V., Beghein, N., Gallez, B., 2003. Nitric oxide-mediated increase in tumor blood flow and oxygenation of tumors implanted in muscles stimulated by electric pulses. Int. J. Radiat. Oncol. Biol. Phys. 55, 1066–1073.

Kwon, G.S., 2002. Block copolymer micelles as drug delivery systems. Adv. Drug Deliv. Rev. 54, 169–190.
Lapenna, S., Giordano, A., 2009. Cell cycle kinases as therapeutic targets for cancer. Nat. Rev. Drug Discov. 8, 547–566.
Lin, R., Connolly, P.J., Huang, S., Wetter, S.K., Lu, Y., Murray, W.V., Emanuel, S.L., Gruninger, R.H., Fuentes-Pesquera, A.R., Rugg, C.A., Middleton, S.A., Jolliffe, L.K., 2005. 1-Acyl-1H-[1,2,4]triazole-3,5-diamine analogues as novel and potent anticancer cyclin-dependent kinase inhibitors: synthesis and evaluation of biological activities. J. Med. Chem. 48, 4208–4211.
Maeda, H., Bharate, G.Y., Daruwalla, J., 2009. Polymeric drugs for efficient tumor-targeted drug delivery based on EPR-effect. Eur. J. Pharm. Biopharm. 71, 409–419.
Mason, K.A., Hunter, N.R., Raju, U., Ariga, H., Husain, A., Valdecanas, D., Neal, R., Ang, K.K., Milas, L., 2004. Flavopiridol increases therapeutic ratio of radiotherapy by preferentially enhancing tumor radioresponse. Int. J. Radiat. Oncol. Biol. Phys. 59, 1181–1189.
Mathot, F., des, Rieux.A., Arien, A., Schneider, Y.J., Brewster, M., Préat, V., 2007. Transport mechanisms of mmePEG750P(CL-co-TMC) polymeric micelles across the intestinal barrier. J. Control. Release 124, 134–143.
Mosmann, T., 1983. Rapid colorimetric assay for cellular growth and survival: application to proliferation and cytotoxicity assays. J. Immunol. Methods 65, 55–63.
Nicolaou, K., Dai, W.-M., Guy, R.K., 2009. Chemistry and biology of Taxol. Angew. Chem. Int. Ed. Eng. 33, 15–44.
Ould-Ouali, L., Ariën, A., Rosenblatt, J., Nathan, A., Twaddle, P., Matalenas, T., Borgia, M., Arnold, S., Leroy, D., Dinguizli, M., Rouxhet, L., Brewster, M., Préat, V., 2004. Biodegradable self-assembling PEG-copolymer as vehicle for poorly water-soluble drugs. Pharm. Res. 21, 1581–1590.
Owens III, D.E., Peppas, N.A., 2006. Opsonization, biodistribution, and pharmacokinetics of polymeric nanoparticles. Int. J. Pharm. 307, 93–102.
Pirollo, K.F., Chang, E.H., 2008. Does a targeting ligand influence nanoparticle tumor localization or uptake? Trends Biotechnol. 26, 552–558.
Pourcelle, V., Devouge, S., Garinot, M., Préat, V., Marchand-Brynaert, J., 2007. PCL-PEG-based nanoparticles grafted with GRGDS peptide: preparation and surface analysis by XPS. Biomacromolecules 8, 3977–3983.
Rapoport, N., 2008. Physical stimuli–responsive polymeric micelles for anti-cancer drug delivery. Prog. Polym. Sci. 32, 962–990.
Schiff, P.B., Horwitz, S.B., 1980. Taxol stabilizes microtubules in mouse fibroblast cells. Proc. Natl. Acad. Sci. U.S.A. 77, 1561–1565.
Schwartz, G.K., Ilson, D., Saltz, L., O'Reilly, E., Tong, W., Maslak, P., Maslak, P., Perkins, P., Stoltz, M., Kelsen, D., 2001. Phase II study of the cyclin-dependent kinase inhibitor flavopiridol administered to patients with advanced gastric carcinoma. J. Clin. Oncol. 19, 2157–2170.
Schwartz, G.K., O'Reilly, E., Ilson, D., Saltz, L., Sharma, S., Tong, W., Maslak, P., Stoltz, M., Eden, L., Perkins, P., Endres, S., Barazzoul, J., Spriggs, D., Kelsen, D., 2002. Phase I study of the cyclin-dependent kinase inhibitor flavopiridol in combination with Paclitaxel in patients with advanced solid tumors. J. Clin. Oncol. 20, 2157–2170.
Sedlacek, H.H., 2001. Mechanisms of action of flavopiridol. Crit. Rev. Oncol. Hematol. 38, 139–170.
Shah, M.A., Schwartz, G.K., 2003. Cyclin-dependent kinases as targets for cancer therapy. Cancer Chemother. Biol. Response Modif. 21, 145–170.
Taper, H.S., Woolley, G.W., Teller, M.N., Lardis, M.P., 1966. A new transplantable mouse liver tumor of spontaneous origin. Cancer Res. 26, 143–148.
Wong, J., Brugger, A., Khare, A., Chaubal, M., Papadopoulos, P., Rabinow, B., Kipp, J., Ning, J., 2008. Suspensions for intravenous (IV) injection: a review of development, preclinical and clinical aspects. Adv. Drug Deliv. Rev. 60, 939–954.
Zhang, J., Yang, P.L., Gray, N.S., 2009. Targeting cancer with small molecule kinase inhibitors. Nat. Rev. Cancer 9, 28–39.